

A practical approach to wave energy modeling and control

Ryan G. Coe ^{1,1}, Giorgio Bacelli ², and Dominic Forbush ²

¹Sandia National Laboratories

²Affiliation not available

November 8, 2023

Abstract

The potential for control design to dramatically improve the economic viability of wave energy has generated a great deal of interest and excitement. However, for a number of reasons, the promised benefits from better control designs have yet to be widely realized by wave energy devices and wave energy remains a relatively nascent technology. This brief paper summarizes a simple, yet powerful approach to wave energy dynamics modeling, and subsequent control design based on impedance matching. Our approach leverages the same concepts that are exploited by a simple FM radio to achieve a feedback controller for wave energy devices that approaches optimal power absorption. If fully utilized, this approach can deliver immediate and consequential reductions to the cost of wave energy. Additionally, this approach provides the necessary framework for control co-design of a WEC, in which an understanding of the control logic allows for synchronous design of the device control system and hardware.

A practical approach to wave energy modeling and control

Ryan G. Coe^{a,*}, Giorgio Bacelli^a and Dominic Forbush^a

^aSandia National Laboratories, Albuquerque, NM, USA

ARTICLE INFO

Keywords:

wave energy converter (WEC)
impedance matching
control

ABSTRACT

The potential for control design to dramatically improve the economic viability of wave energy has generated a great deal of interest and excitement. However, for a number of reasons, the promised benefits from better control designs have yet to be widely realized by wave energy devices and wave energy remains a relatively nascent technology. This brief paper summarizes a simple, yet powerful approach to wave energy dynamics modeling, and subsequent control design based on impedance matching. Our approach leverages the same concepts that are exploited by a simple FM radio to achieve a feedback controller for wave energy devices that approaches optimal power absorption. If fully utilized, this approach can deliver immediate and consequential reductions to the cost of wave energy. Additionally, this approach provides the necessary framework for control co-design of a wave energy converter, in which an understanding of the control logic allows for synchronous design of the device control system and hardware.

1. Introduction

Ocean waves are an attractive renewable energy resource. Firstly, the size of the resource is considerable. While estimates vary somewhat, the global wave resource is on the order of 2 TW when one considers the average annual power arriving at coastlines [1] - the resource may be perhaps an order of magnitude larger if the general oceans beyond the coastlines are considered. To put this in perspective, as of 2015, the CIA estimated average world electrical power production to be roughly 2.7 TW [2]. (On average 14% of this 2.7 TW is attributed to renewable sources other than hydroelectric dams.) The United States' share of the wave power resource amounts to some 200 GW on average [1, 3], with US average power usage in 2016 being roughly 450 GW [2].

Another compelling quality of ocean waves is their proximity to population centers. Roughly half of the world's population, some 4 billion people, live within 100 km of the coast [4]. This figure is even more impressive when one considers that this coastal area accounts for perhaps 1/10th of the world's land mass. For the wave energy developer and the electrical utility operator alike [5, 6], considering the costs and losses associated with long distance electrical transmission, the proximity of the ocean wave resource to human population centers provides another compelling argument for pursuing wave energy generating technologies.

Another factor is that the predictability of ocean waves is generally very good, with high accuracy predictions possible on the scale of days [7]. This follows from the fact that swells, which, after being generated by wind at some distant location, travel coherently over long distances, tend to contain a large fraction of wave energy. Predictability is a particularly attractive quality when considering the modern electrical grid, with its many varied generation sources, loads, and storage requirements [8, 9].

Certainly there are many compelling arguments for pursuing devices to generate electricity from ocean waves. At a basic level designing such a device is relatively easy. The challenge, of course, lies in designing a wave energy converter (WEC) that can produce electricity at a cost-competitive rate. While estimates vary widely, the levelized cost of energy (LCOE) – that is the cost of electricity excluding any government incentives – achieved by a WEC is on the order of 1-0.5 \$/kWh [10–12]. To be competitive with other grid-scale generation technologies, such as natural gas and wind, the cost of wave energy must drop by at least half to be feasible in some high-cost energy markets (e.g., islands), and by a factor of 10 to be more broadly practical.

Sandia National Laboratories is a multi-mission laboratory managed and operated by National Technology and Engineering Solutions of Sandia, LLC., a wholly owned subsidiary of Honeywell International, Inc., for the U.S. Department of Energy's National Nuclear Security Administration under contract DE-NA0003525. This paper describes objective technical results and analysis. Any subjective views or opinions that might be expressed in the paper do not necessarily represent the views of the U.S. Department of Energy or the United States Government.

*Corresponding author

 rcoe@sandia.gov (R.G. Coe); gbacell1@sandia.gov (G. Bacelli); dforbus@sandia.gov (D. Forbush)
ORCID(s): 0000-0003-0738-3772 (R.G. Coe); 0000-0002-1208-2352 (G. Bacelli)

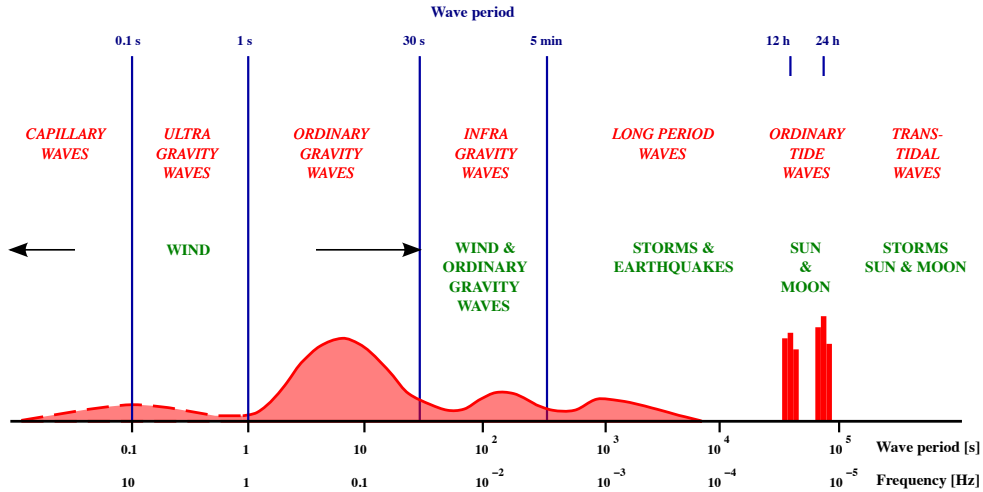


Figure 1: Spectral distribution of ocean waves, redrawn from [19] (by Mikhail Ryazanov, licensed by CC BY 3.0 / units abbreviated).

Many studies point to the design of better controllers as a major, if not the critical, pathway for improving the economic viability of WECs [12–14]. The belief in the potential for better control strategies to deliver a cost competitive WEC has taken on an almost mystical aura, with studies reporting increases in energy by many fold [15, 16]. The promise of control design’s potential to improve WEC performance has been around for at least 40 years (see, e.g., [17, 18]). However, we have yet to see commercially successful WECS.

This study presents a process for modeling and model-based control design that can readily be applied to improve the performance of WECs. These methods additionally provide intuitive insights to the designer, which support further innovation through control co-design. After a brief discussion on some key aspects of the wave energy resource, the usage of impedance models to capture WEC dynamics is explained and demonstrated. Based on these impedance models and an understanding of the wave resource, we can design feedback controllers based on an impedance matching approach. These simple controllers are shown to provide performance that approaches the theoretical limit.

2. The wave energy resource

While quantification and characterization of the wave energy resource has and should continue to receive substantial attention, for the purposes of this paper we can consider just two aspects of the resource. The design of a WEC is essentially the design of an oscillator. With this in mind, we should want to know something about the input to that oscillator.

First, we should want to know *where* the energy input to the oscillator occurs, in terms of the frequency. Figure 1, illustrates the spectral distribution of energy in water waves. Here, we can see that the energy of interest (the “ordinary gravity waves” in Figure 1) ranges from $1 < T < 30$ s. Even this range is relatively conservative, and the bounds can be drawn as perhaps $5 < T < 20$ s.

The second question of interest at this stage is how broadly the energy is distributed at any given time and location. The well used Bretschneider spectrum, which represents a fully-developed sea (i.e., waves that have previously been generated by wind and are no longer being augmented), provides a nice illustration. A Bretschneider spectrum with a peak period of $T_p = 8$ s has an energy period of $T_e = 6.9$ s; roughly 80% of the energy in this sea state is located in the range $5 < T < 10$ s ($0.1 < f < 0.2$ Hz). The sea state will change appreciably, resulting in some shift of the spectral energy, only over the course of hours. While the Bretschneider spectrum is a very basic approximation of real ocean waves, which in practice are often not “fully developed,” or may have some bimodal characteristic, the general conclusion about the narrowness of the energy distribution stands [20].

To put the spectral width of ocean waves into perspective, we can consider other engineered oscillators. Table 1 shows the spectral ranges of some human-engineered systems along with a number of evolution-engineered systems. For example, we can see from Table 1 that TV antennas are designed to handle waves ranging an entire order of

Table 1
Spectral width of different oscillators.

System	Frequency range
US broadcast television	54-700 MHz
AM radio	0.6-1.6 MHz
Visible light	430-750 THz
Audible sound	20-20,000 Hz
Gravity water waves	0.05-1 Hz
Individual sea state (example)	0.1-0.2 Hz

magnitude (one decade). The human ear is capable of oscillating in waves spanning three decades (see “audible sound” in Table 1). The International Telecommunication Union (ITU) divides the radio spectrum into bands, each covering a decade of frequencies. For example, the Ultra Low Frequency (ULF) band spans $300 < f < 3,000$ Hz, the Very Low Frequency (VLF) band spans $3,000 < f < 30,000$ Hz, and so on.

Taking all these other systems into perspective, the range of a Bretschneider sea state (much less than half a decade) is indeed relatively narrow. Even the entirety of ocean gravity waves span just more than one decade of frequencies. As will be discussed in the subsequent sections, this is a very attractive characteristic when engineering a WEC.

3. Collecting wave energy

With few exceptions,¹ WECs are well described as resonant systems. In fact, the simple spring-mass-damper so familiar from many physics and engineering textbooks (see, e.g., [21–23]) – and minor logical extensions thereof – provides a remarkably potent model for a WEC. This idea is, of course, not new (see, e.g., [18, 24–27]). However, it seems that the power of using spring-mass-damper framework for the modeling of a WEC has not yet fully been realized.

3.1. A realistic, practical, and powerful WEC model

Figure 2 illustrates a progression to model a WEC as a spring-mass-damper. Working from left to right, we start on the far left with a floating body having a mass, m . The dynamics of this system can be well replicated by the spring-mass-damper shown in the center tile of Figure 2, where the hydrostatic stiffness and wave radiating effects of the body have been replaced by a spring, K_{HS} , and a damper, $B(\omega)$, respectively, with an additional (“added”) mass, $A(\omega)$. An additional damping term, B_f is also shown in the center tile of Figure 2 to account for friction (e.g., due to viscosity). The excitation force created by incoming waves is represented by an external input, F_e .

The right-hand tile of Figure 2 progresses from a floating body to a WEC by including additional spring and damper components to represent a power take-off (PTO). The damper component of the PTO, $B_{pto}(\omega)$, has parallels in other mechanical generation technologies. To convert mechanical power to electrical power, the generator must apply a “braking” torque (i.e., a damping) that resists the velocity of the input shaft, which is driven by the energy source. The amount of energy extracted is equal to the amount of mechanical work done by the generator on the input shaft minus losses. Fundamentally speaking, this is no different from the generator in a hydroelectric dam, a wind turbine, or nuclear power plant – the energy source provides some input torque, and the generator imparts a damping reaction to extract electrical power.

The spring component of the WEC PTO, $K_{pto}(\omega)$, does not have the same direct analogs in other energy generation technologies. The need for this spring component stems from the intrinsic nature of a WEC: it is an oscillating body. Other mechanical energy generation technologies effectively harness a DC input force (e.g., the mostly constant torque produced by a wind turbine in a constant breeze with gusts and turbulence creating only small disturbances). Since, in a WEC, we must *tune* a resonator, the inclusion of some tunable spring is only logical. In many ways, this departure from the mode of operation of existing energy generation technologies represents a central challenge that has impeded the development of commercially viable WECs.

However, there are other useful analogues to understand the spring component within the WEC PTO representation in the right-hand tile of Figure 2. Maximizing power transfer between oscillatory systems is actually a fairly old, and

¹Most notably, “overtopping” devices are not generally designed to operate as resonant bodies.

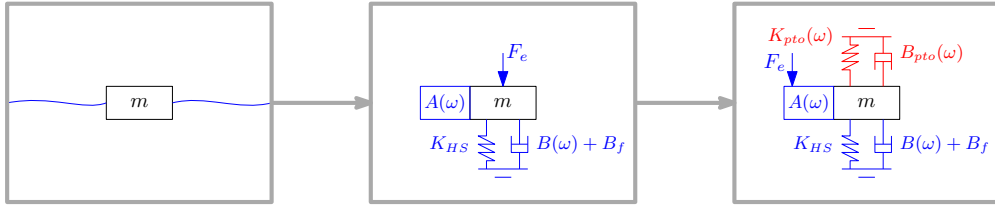


Figure 2: A progression to represent a WEC with a composite spring-mass-damper (left: floating body; middle: wave-body interaction replaced by a spring-mass-damper; right: WEC PTO represented by a spring-mass-damper).

well-understood, problem. The original application area for this concept was electrical power distribution lines, where engineers needed to maximize the transfer of AC power throughout the electrical grid. At the end of a transmission line, a transformer must convert the voltage of an AC signal. The problem faced by engineers designing electrical power distribution systems is thus surprisingly similar to that for the designer of a WEC. Instead of two electrical AC systems, the WEC designer must consider energy transfer for the ocean waves to the WEC body.²

Fortunately for the WEC designer, electrical engineers have provided the concept of “impedance matching,” which enables maximum power transfer in such an interaction [29, 30]. Impedance is a term generally well-known amongst mechanical engineers, but the quantity is effectively a measure of the opposition to motion or “flow” when a “potential” is applied; it can be calculated as the ratio of “potential” to “flow.” Electrically, this could be the ratio of voltage to current (voltage is the “potential,” current is the “flow”); mechanically, we can quantify the ratio of force to velocity via an impedance (force is the “potential,” velocity is the “flow”). In fact, the framework of impedance modeling is applied to many applications beyond electronics, including prosthetics, automotive suspensions, and earthquake rated structures.

For a WEC, we can derive a description for the wave-body interaction in terms of impedance by starting from Newton’s second law.

$$\begin{aligned} m a(t) &= \sum f(t) \\ &= f_r(t) + f_h(t) + f_f(t) + f(t) \end{aligned} \quad (1)$$

Here, m and a are the mass and acceleration of the floating body, respectively. The forces acting on the body have been decomposed (assuming linear superposition) into the radiation component, f_r , which represents the force due to waves induced by body motions; a hydrostatic component, f_h , representing the balance between gravity and buoyancy; a friction force, f_f ; and a component to account for other external forces, f . Because of the oscillatory nature of waves, it is convenient to work in the frequency domain, where the independent variable is the angular frequency ω . The resulting model is (see, e.g., [25, 31])

$$m i\omega V(\omega) = -(B(\omega) + i\omega A(\omega)) V(\omega) - \frac{K_{HS}}{i\omega} V(\omega) - B_f V(\omega) + F(\omega), \quad (2)$$

where $V(\omega)$ is the velocity, i is the imaginary unit, and we have applied the Fourier transform differentiation property to write the acceleration in terms of the velocity as $\mathcal{F}[a(t)] = i\omega V(\omega)$. Note also that upper case variables are used in (2) to indicate these terms are all in the frequency domain. The Fourier transform of the radiation, hydrostatic and friction forces are

$$F_r(\omega) = -(B(\omega) + i\omega A(\omega)) V(\omega) \quad (3a)$$

$$F_h(\omega) = -\frac{K_{HS}}{i\omega} V(\omega) \quad (3b)$$

$$F_f(\omega) = -B_f V(\omega). \quad (3c)$$

²In truth, the goal must be to transfer energy from the ocean waves, to the WEC body, to the electrical generator, and to electrical power. This concept and means of analysis are discussed in [28].

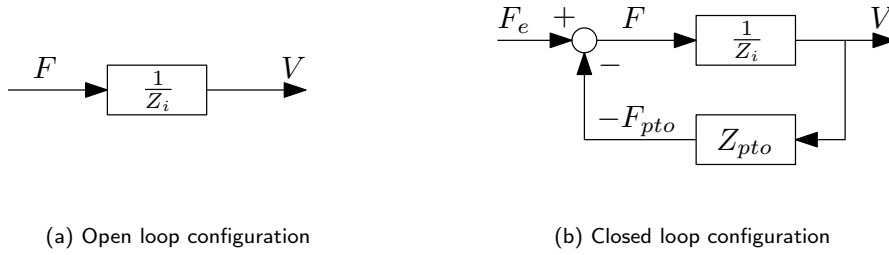


Figure 3: Equivalent block diagrams of a WEC.

The relation between the applied external force and the resulting velocity, that is the impedance $Z_i(\omega)$, can now be written by rearranging (2).

$$V(\omega) = \frac{F(\omega)}{B(\omega) + B_f + i \left(\omega(m + A(\omega)) - \frac{K_{HS}}{\omega} \right)} = \frac{F(\omega)}{Z_i(\omega)} \quad (4)$$

where $Z_i(\omega) = B(\omega) + B_f + i \left(\omega(m + A(\omega)) - \frac{K_{HS}}{\omega} \right)$

In the field of control theory, it is very common to use block diagrams to study the connection of multiple systems and (4) can be considered as the open loop configuration of a WEC, as depicted in Figure 3a, where the input is the force F and the output is the velocity V . The dynamics of system are described by the inverse of the intrinsic impedance $1/Z_i$.

Now we must consider the term $F(\omega)$ in (4). Returning to the center pane of Figure 2, we can account for the wave excitation force, $F_e(\omega)$, with this external forcing term.

$$V(\omega) = \frac{F_e(\omega)}{Z_i(\omega)} = \frac{F_e(\omega)}{B(\omega) + i \left(\omega(m + A(\omega)) - \frac{K_{HS}}{\omega} \right)} \quad (5)$$

Continuing the progression in Figure 2 to the far right pane, we can represent the force of the PTO, with its damper (B_{pto}) and spring (K_{pto}) components, as

$$F_{pto}(\omega) = - \left(B_{pto} - \frac{i}{\omega} K_{pto} \right) V(\omega). \quad (6)$$

Recalling again that impedance can relate force and velocity in a mechanical system, we can revise (6) into a form based on a PTO impedance, Z_{pto} .

$$F_{pto}(\omega) = -Z_{pto}(\omega)V(\omega)$$

where $Z_{pto}(\omega) = B_{pto} - \frac{i}{\omega} K_{pto}$ (7)

Considering the block diagram in Figure 3a, the definition in (7) shows that the PTO force depends on the output of the system, which is the velocity V . In this case, the WEC is in a closed loop configuration because its input depends on the output by mean of a feedback branch, given by the path connecting the velocity with the input force through the PTO impedance, as shown in Figure 3b. The negative sign in the input summing block is used to be consistent with the classical control theory, where feedback is generally negative; in this way it is immediately possible to the wide range of tools already available for analysis and control design.

The model for the closed loop system can be easily derived by substitution of the PTO force definition (7) into (4) to give us a representation for the WEC shown in the right most pane of Figure 2.

$$V(\omega) = \frac{F_e(\omega) + F_{pto}(\omega)}{Z_i(\omega)} = \frac{F_e(\omega)}{Z_i(\omega) + Z_{pto}(\omega)} \quad (8)$$

With an impedance model for the WEC given by (4) and the understanding that impedance matching will provide maximum power transfer from the waves to the PTO damper, we can find the optimal values for $B_{pto}(\omega)$ and $K_{pto}(\omega)$. The details of this process are excluded here for brevity, but thorough explanations are provided in [25, 28]. The result is that an optimal PTO can be obtained by setting the PTO impedance as

$$Z_{pto}(\omega) = Z_i^*(\omega), \quad (9)$$

where the symbol * represents the complex conjugate. For the damping and stiffness terms shown in the far right pane of Figure 2, this simplifies to

$$\begin{aligned} B_{pto}(\omega) &= \Re\{Z^*(\omega)\} \\ &= B(\omega) \end{aligned} \quad (10a)$$

$$\begin{aligned} K_{pto}(\omega) &= \omega \Im\{Z^*(\omega)\} \\ &= -\omega \Im\{Z(\omega)\} \\ &= -\omega^2 (m + A(\omega)) + K_{HS}. \end{aligned} \quad (10b)$$

If one attempts to set B_{pto} and K_{pto} so as to follow (10), the resulting control system will be acausal, meaning that the optimal control input *now* depends on the velocity in the *future* (more on this in Section 3.3). However, further consideration of realistic ocean waves and a realistic WEC (i.e., how the function $Z(\omega)$ might be shaped) shows that the situation may not be so dire after all.

3.2. How does a WEC impedance look?

At this stage, it is useful to consider some practical examples to better understand the application of impedance modeling for a WEC. Figure 4 depicts two devices that are presented as examples herein. Figure 4a shows the “WaveBot,” which is a point absorber capable of motion in heave, surge, and pitch [32]. In this example, we consider the heave mode of the WaveBot in isolation. Figure 4b shows the “floating oscillating surge wave energy converter (FOSWEC),” which has two pitching flaps – one at “bow” and one at the “aft” – normal to the wave propagation direction [33]. These devices have both been experimentally tested and the ensuing models are produced via system identification (SID) methods [34–36]. Note that models can similarly be produced based on numerical tools such as WAMIT [37] and Nemoh [38].

A series of photographs from the tests of each device are shown in Figure 5. The top series (Figure 5a-5d) shows the WaveBot. The lower series (Figure 5e-5h) shows the FOSWEC. Note that both WaveBot and FOSWEC are scaled devices, designed to operate in the waves that can be realistically produced within the basin where they are tested. For the WaveBot, which is tested in the Navy’s Maneuvering and Sea Keeping (MASK) basin, waves with $T < 6$ s are possible. The FOSWEC is tested in the smaller Oregon State University (OSU) O.H. Hinsdale Wave Research Laboratory (HWRL) Directional Wave Basin (DWB), which can generally handle waves with $T < 4$ s.

We can test the assertion that a spring-mass-damper should serve as our fundamental model for a WEC by considering experimental data for the WaveBot and FOSWEC. Figure 6 shows a Bode plot³ of two models WaveBot’s impedance. The blue curve in Figure 6 shows a nonparametric model of the WaveBot’s impedance obtained from wave tank data; the red curve is a 2nd-order transfer function of the form

³Bode plots are a powerful tool for analyzing system dynamics; the upper axes show the magnitude (in decibels) and the lower axes show phase. The frequency is shown in log form on the horizontal axis.

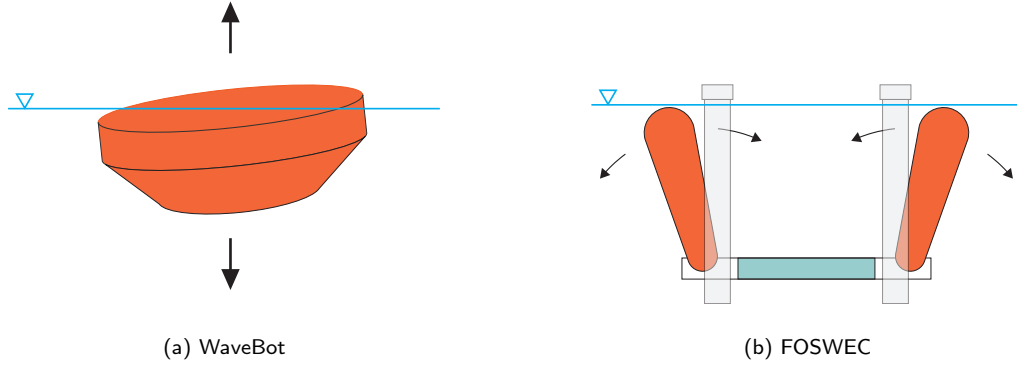


Figure 4: Wave energy devices considered herein. Arrows show degrees-of-freedom.

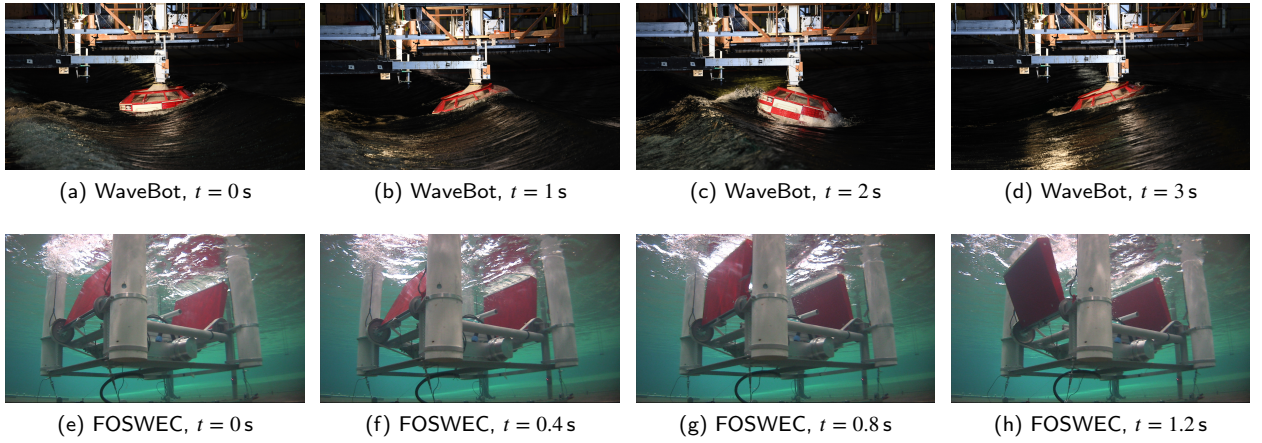


Figure 5: WaveBot (top) and FOSWEC (bottom) in motion.

$$Z(\omega) = k \frac{(i\omega)^2 + b_1 i\omega + b_0}{i\omega}. \quad (11)$$

Not so incidentally, (11) is the velocity-to-force frequency response of a spring-mass-system (see, e.g., sec. 6.3 in [23]). Thus, we can see from Figure 6 that the impedance of the WaveBot is very well captured by this spring-mass-damper model (in fact, with a fit of 85%).

Moving on to the FOSWEC, we find the story to be somewhat more complicated, but nonetheless similarly themed. While the heave motion of the WaveBot is sufficiently decoupled from the pitch and surge motions to be considered independently, the two flaps of the FOSWEC are strongly coupled and must therefore be considered simultaneously. Thus, Figure 7 shows the multi-input, multi-output (MIMO) FOSWEC impedance. As with the WaveBot, a Bode plot is used to display the impedance models for the FOSWEC. However, since the FOSWEC is a MIMO system with two inputs and two outputs (one each for the bow and aft flaps), Figure 7 contains four sets magnitude and phase plots – mathematically, we can write $Z_{i,j}(\omega) = F_j(\omega)/V_i(\omega)$ to define these four components of the MIMO impedance model.

The diagonal impedances shown in Figure 7 (i.e., the pairs in the upper left and lower right corners) represent self-reaction. For example, the upper left plots correlate to the torque of the aft flap motor required to create a velocity on the aft flap. The off-diagonal terms (i.e., the pairs in the upper right and lower left corners) represent coupling between the flaps. These coupling effects account for how one flap affects the other (e.g., the upper right plots correlate to torque required from the bow motor to create a velocity on the aft flap). Closer observation reveals just how strongly the two flaps affect each other: the off-diagonal impedance magnitudes are only roughly 0.2 dB lower than the diagonals (i.e.,

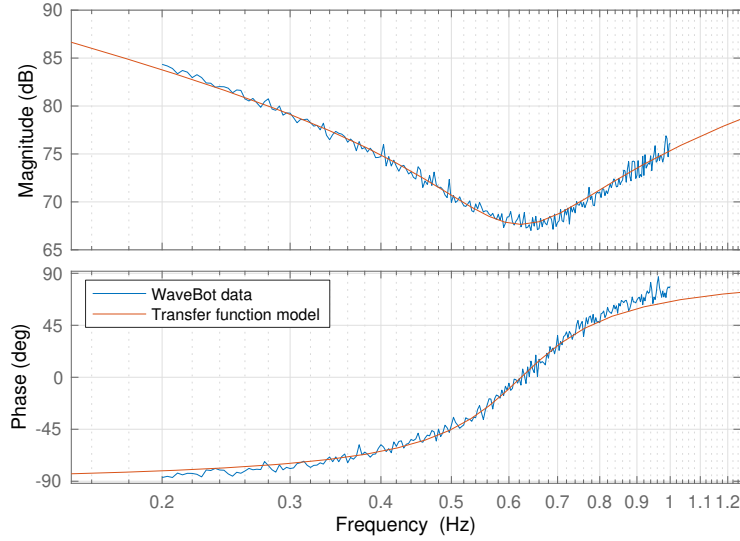


Figure 6: Bode plot showing a 2nd-order transfer function to approximate the impedance of the WaveBot wave energy converter (fit: 85%).

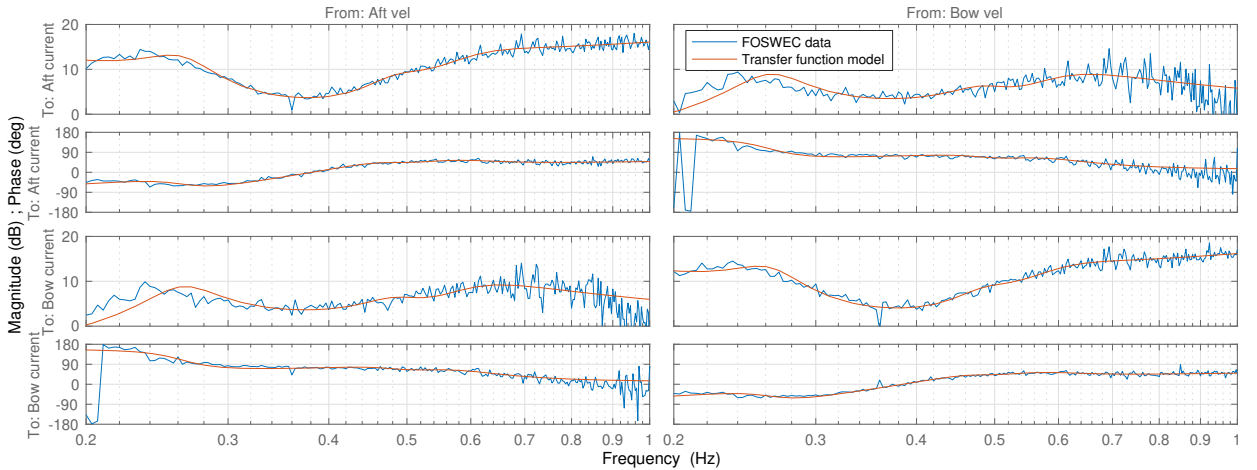


Figure 7: Bode plot showing 5th-order transfer functions to approximate the impedances of the FOSWEC (fits: [79 72; 73 79]%).

the cross coupling impedance is 95% as important as the direct impedance).

In addition to the need to consider the coupling effects between the FOSWEC's flap via a MIMO system, a higher order transfer function has also been used. Whereas a 2nd-order transfer function model captured the WaveBot's impedance well, 5th-order models have been used for each of the four FOSWEC impedances. Thus, while the FOSWEC device is indeed more complex and no longer fits so cleanly into a single spring-mass-damper analog, the impedance model can again accurately represent the device's dynamic (in this case to within better than 70%).

With accurate impedance models for the WaveBot and FOSWEC, the path to designing a controller to maximize power transfer from the waves to the WEC is straightforward based on (10). We must simply set $B_{pto}(\omega) = \Re\{Z^*(\omega)\}$ and $K_{pto}(\omega) = \omega \Im\{Z^*(\omega)\}$. However, this results in an acausal controller (i.e., the PTO force is dependent on the future velocity). Before we move too quickly to the task of predicting the future, we can further examine this issue of acausality.

3.3. Acausality

A great deal has been written about acausality in the field of wave energy. The concept of acausality – that we must know the future in order to make a decision about the present – can be quite impressive and impactful, and it seems to have had an out-sized influence on research within the field of WEC control design. The subsequent sections provide some clarity on this issue and its implications to WEC control design. There are two components of acausality when we consider modeling and control of a WEC: excitation and optimal impedance matching. Examining each of these in turn can clarify their real consequences for the engineering of a WEC.

3.3.1. Acausality: excitation

Firstly, we can consider acausality as it relates to the excitation of a WEC by the ocean waves. This system is acausal only when viewed from a specific perspective, but otherwise the physics, as with all other Newtonian physics, are strictly causal. The perspective in this case is a matter of what you consider as the *cause* of the excitation to the WEC.

If we consider, as is most often done, that the wave elevation (i.e., the disturbance in the level of the ocean's free surface) at the center of the device is the cause of the excitation, then we find that the excitation process is acausal. This implies that we must have foreknowledge, through some combination of “up-wave” measurement, propagation, and modeling, of the wave elevation in the future to know the excitation on the WEC now. The problem with this approach is again the selection of the wave elevation as the source of the excitation.

In fact, the excitation is caused by the particle velocities beneath the water's surface, which in turn impart a pressure onto the WEC's hull.⁴ If we were to use these velocities as the input to our system, a causal excitation model would result. As has been shown in [34], using a measurement of pressure as an input also results in a causal excitation model. Thus, this source of acausality is really a figment of our common engineering and modeling construct – since it is easier to measure wave elevation than particle velocity, we wind up with an acausal excitation model.

3.3.2. Acausality: impedance matching

As discussed in Section 3.1, the impedance matching controller suggested by (10) results in an acausal system. Unlike the preceding discussion of excitation in Section 3.3.1, this outcome is not a matter of perspective. In fact, this outcome is not at all limited to wave energy. For any causal system, the complex-conjugate of the impedance will produce an acausal system (see sec. 3.1.1 of [39]). Thus, as our WEC is a causal system, when we take the complex conjugate of the WEC impedance, we must arrive at an acausal system. In other words, to implement (10) perfectly across all frequencies, you must know what will happen to the WEC in the future (i.e., the controller implementation will be acausal).

This outcome of an acausal controller sounds fairly troublesome. However, as discussed in Section 3.1, the concept of impedance matching for maximum power transfer is borrowed from electrical engineering. In order to make the electric grid function and to tune the radio in your car, an *engineering solution*, in which assumptions and sacrifices are made to obtain a viable result, has already been devised. If we can agree that our controller must work well only over some finite range of frequencies, and that it does not instead need to operate perfectly at all frequencies simultaneously, the situation becomes more favorable.

3.4. Causal realization

There is in fact no need for our controller to perform perfectly at all frequencies simultaneously. From Section 2, we know that the energy in a typical sea state ranges over at most a single decade of frequencies, with the sea state changing appreciably only over the course of hours. This key piece of information (the band-limited and slowly varying nature of ocean waves) allows us to utilize a causal realization of the impedance matching approach. If we manage, for some limited frequency range covering – or nearly covering – the frequency range of the incoming ocean waves, to approximate the complex conjugate of the WEC impedance, we may achieve a satisfactory result.

When considering a limited frequency band, approximating the complex conjugate of the impedance turns out to be relatively simple. The frequency response of the well-known proportional-integral-derivative (PID) controller is

⁴Note that, returning to (4), we have linearized the wave-body interaction dynamic and thus decoupled the interaction between the hull and the free surface, which is represented f_h , from the interaction between the hull and the waves, which is represented by f_e . See, e.g., [31] for a complete discussion of linear hydrodynamics.

[21, 23]

$$C_{PID}(\omega) = \frac{(i\omega)^2 K_D + i\omega K_P + K_I}{i\omega}. \quad (12)$$

Here, K_P , K_D , and K_I are, respectively, the proportional, derivative, and integral gains of the controller. By means of simple manipulation, we see that the PID controller will produce an impedance of the following form:

$$\begin{aligned} Z_{PID}(\omega) &= i\omega K_D + K_P - i\frac{K_I}{\omega} \\ &= K_P + i\left(\omega K_D - \frac{K_I}{\omega}\right). \end{aligned} \quad (13)$$

Comparing (13) to (4), we can notice a striking similarity between the two expressions. The key difference is that the PID is a very simple controller and is characterized by a fairly simple frequency response; in fact it only has three parameters: one for tuning the real part (K_P), and two for tuning the imaginary part (K_I and K_D). This means that the PID controller's impedance will be perhaps less malleable than desired as we try to fit a desired impedance (Z_i^*), but, this shortcoming is not so extreme and, over limited frequency bands of interest, is often acceptable.

Returning again to the WaveBot and FOSWEC examples, it is quite possible to design even a PI controller (dropping the K_D term, which can improve stability in practical applications) that can cover the majority of the energy in a sea state. Figure 8 shows plots illustrating the approximate impedance matching achieved by PI controllers for the WaveBot (Figure 8a) and the FOSWEC (Figure 8b). In each case, PI controllers (shown in red lines) are tuned to best capture the energy in a Bretschneider spectrum with a significant wave height of $H_s = 0.127$ m and a peak period of $T_p = 3$ s (recall again that the WaveBot and FOSWEC are model-scale devices, hence the selection of this small wave sea state). Along with the PI controllers, proportional ("P") resistive damping controllers are shown (magenta lines). The ideal complex conjugate impedance matching controllers are shown (blue lines).

The gray rectangles in Figure 3 illustrate the key region of excitation forcing (F_e) caused by the incoming waves. The rectangle illustrates the frequency range in which $F_e \geq \frac{1}{2} \max(F_e)$, and is thus the region in which the impedance match should be at its best. We can see from Figure 3 how the impedance created by the PI controllers approximate that of the perfect impedance matching in the region with the highest level of excitation forcing. While it is clear that the impedances produced by the PI controllers are far from perfect, the power produced by these controllers is a much better measure of their utility.

The performance of these controllers is illustrated by Figure 9. Figure 9a depicts the performance of the WaveBot with a PI controller in the selected sea state. First, we can see the excitation force wave power, F_e (gray). Below this, are three normalized power area curves representing the power generated by different controllers: the first shows the optimal theoretical power (this cannot be achieved in practice) achieved with perfect impedance matching (blue), the second shows the PI controller tuned to achieve a causal approximation of the complex conjugate control (red), and the third shows the P controller (magenta). From Figure 9a, it is clear to see that PI controller does a very good job of approximating the complex conjugate control, as it returns roughly 93% of the theoretical maximum power.

The same approach for causal impedance matching controller design can also be applied to the FOSWEC, as shown in Figure 9b. In addition to its multiple degrees of freedom, another interesting aspect of the FOSWEC is that, as with most flapping WECs, it has a relatively low resonant frequency (roughly 0.4 Hz in this case). As we can see from Figure 9b, the energy frequency of the wave spectrum is very nearly aligned with the natural frequencies of the FOSWEC's flaps. Again, the PI controller designed for the FOSWEC in this sea state approaches limit of maximum power absorption, if not quite as closely as with the WaveBot. The lower performance of the PI controller for the FOSWEC versus the WaveBot can be partially attributed to the wide bandwidth of the FOSWEC (note from Figure 8b that the shaded excitation region of the FOSWEC spans a much broader frequency range).

There are two key factors that can work to degrade the effectiveness of the causal impedance matching approach outlined in this paper: broadband waves and nonlinearity of the WEC dynamic system. As discussed in Section 2, the wave energy resource is relatively narrow-banded in general. The results in this Section show that PI controllers can match the impedance well over the limited frequency range of an ocean sea state. Much as you might swap the station on your radio to change classical and to rock & roll, altering the tuning of your WEC controller every hour or so to track

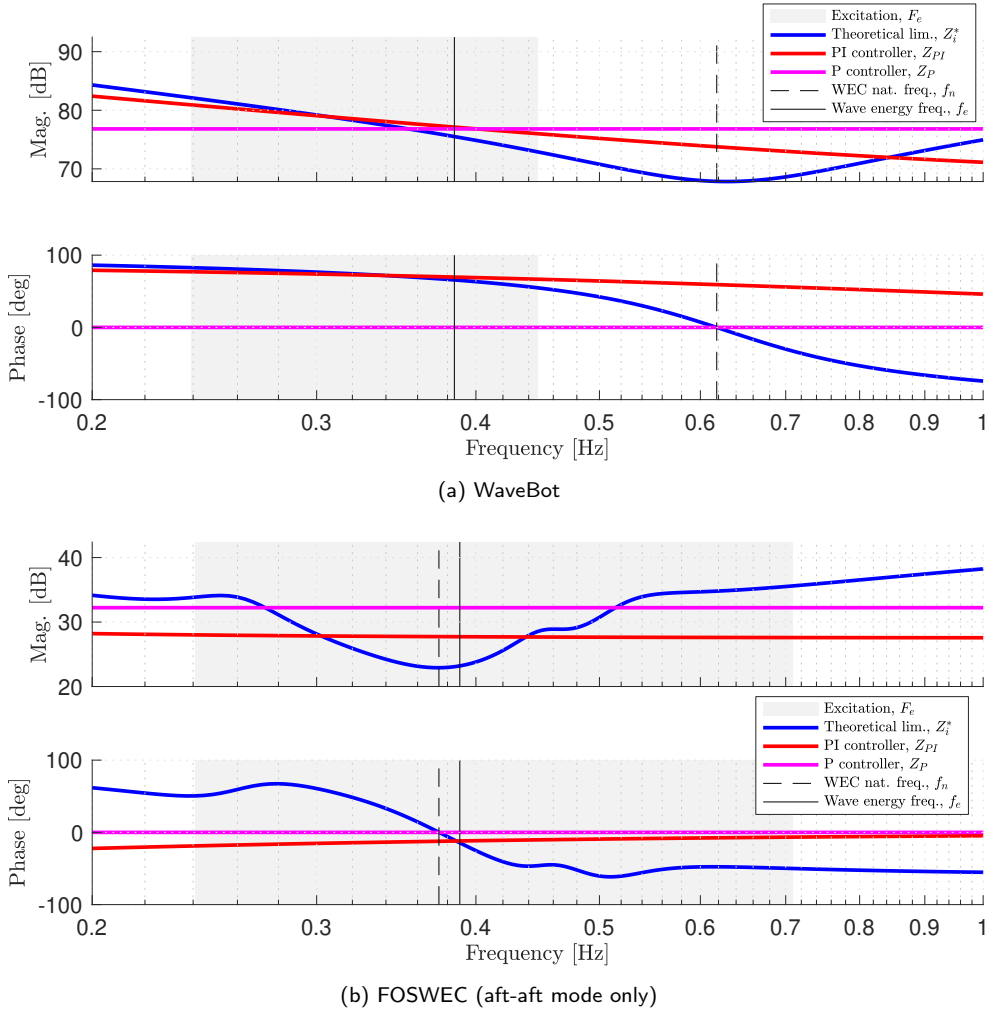


Figure 8: Complex conjugate of impedance (Z^*) and causal impedance matching controllers (Z_{PI}). Region excited by incoming waves ($F_e \geq \frac{1}{2} \max(F_e)$) shown with gray box.

changing sea states is quite tractable (some smaller benefits may even be had by increasing the rate to perhaps every five minutes). This can be achieved by using the WEC impedance model to obtain an estimate of the current sea state based on measurements of the WEC’s velocity and using this for the basis of selecting the appropriate controller gains [40]. Such a control system can employ an optimization scheme to select gains in real-time or a look-up table based on previous analysis, perhaps including some site-specific considerations. Additionally, an interesting logical extension of this approach is that the three gain terms in (12) are by no means the limit, and in fact higher-order controllers such as the Feedback Resonating Controller (FBR) [41, 42] can offer even broader impedance matching and therefore higher levels of power capture. A similar approach has also been presented more recently in [43]. Another consideration, as shown in [44], is that model predictive controllers (MPCs) can be designed to track such feedback controllers in order to handle constraints without any need for wave prediction.

The question of nonlinear dynamics has received significant interest within the WEC community [45–48]. While the complex hydrodynamics of a floating body combined with the dynamics of hydraulic circuits and electrical machines are certainly nonlinear, a practical and effective approach is to apply local linearizations to model systems [49]. Just as the WEC controller can be modulated/scheduled over time to reflect changing sea conditions (“changing the radio station”), the same can be done with the underlying dynamics model. Since sea states change slowly, it is quite practical to, for example, apply one local linear model (“model A”) when $2 < H_s < 3$ m and $4 < T_p < 5$ s, and second

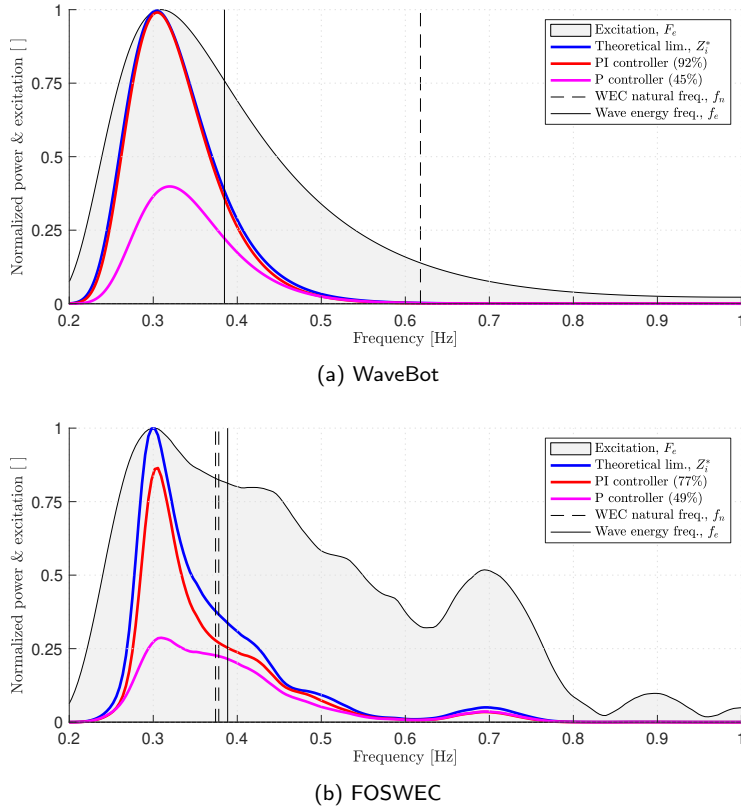


Figure 9: Normalized performance of the WaveBot and FOSWEC in JONSWAP sea state with $H_s = 0.127$ m, $T_p = 3$ s, $\gamma = 1$ for optimal impedance matching (Z_i^*), proportional-integral (PI), and proportional (P) controllers shown with normalized wave excitation spectrum (F_e).

local linear model (“model B”) when $3 < H_s < 4$ m and $4 < T_p < 5$ s. A practical example is shown by Bacelli et al. [34], in which mechanical friction effects within a WEC PTO, which are well-known to exhibit a nonlinear dynamic behavior (see, e.g., [50]), are linearized based on the amplitude of motion.

4. Conclusion

The approach suggested in this paper, of using impedance models to capture WEC dynamics and causal feedback controllers designed based on those impedance models to maximize power absorption, is far from cutting-edge and is based on well-established practices from other engineering fields. In fact, the approach has been identified by previous WEC researchers, including Salter [51], Perdigao and Sarmiento [52], Hals [53] and others [26, 54–56]. Further, despite the relative simplicity of this strategy, causal impedance matching controllers can come quite close to approximating ideal impedance matching over the finite frequency ranges relevant for ocean sea states.

The evidence in support of this approach of impedance modeling and causal impedance matching approximations is quite convincing, and it seems that this manner of WEC design is fully deserving of broad application. For many WECs, a causal impedance matching controller could be immediately implemented and deliver improved performance. Further, the relative simplicity leads to what may be this method’s strongest asset: an intuitive insight for the designer.

An intuitive insight into the functionality of the controller is essential to enabling an engineer to utilize a control co-design approach. The simplification to work with mechanical power was employed in this paper to facilitate a more straightforward explanation and discussion, but electrical power is the real goal for a WEC. As shown by Bacelli and Coe [28], the impedance modeling and matching methods suggested in this paper can be extended to consider real PTO systems. The key challenge in design of a high-performing (cost-competitive) WEC is to design the PTO, as well as remaining hardware, such as hull shape, mooring system, and array power electronics, to achieve symbiosis with

the controller.

This difficult task of designing a cost-effective WEC PTO will be made much easier if the designer has not only an effective and readily implementable controller, but also an intuitive understanding of that controller's function and logic on which to base design decisions. In practice, an engineer could consider whether adding storage in a particular location within the PTO, in the form of either inertia or a spring effect, will bring the entire system's dynamics closer to that goal of impedance matching. Alternatively, a designer can base decisions about PTO gearing, sensor selection, and sensor placement to preserve stability while delivering the level of damping feedback indicated by the real part of the impedance.

Reviewing the work to date and the summary presented in this paper, it is clear that a WEC can be controlled to deliver very good energy absorption by applying the well-established approach principle impedance matching. This approach produces simple, robust controllers for WECs, which can be readily implemented on today's devices using existing sensors and hardware. Additionally, and perhaps more importantly, using an impedance modeling framework and working towards impedance matching provides the designer with concrete analysis tools to improve power absorption throughout many subsystems of a WEC.

Acknowledgments

The authors would like to thank Vincent Neary, Peter Kobos, Jesse Roberts, Kelley Ruehl, Sterling Olson, Bill McShane, and Jeff Rieks for their useful feedback on this paper. Sandia National Laboratories is a multi-mission laboratory managed and operated by National Technology and Engineering Solutions of Sandia, LLC., a wholly owned subsidiary of Honeywell International, Inc., for the U.S. Department of Energy's National Nuclear Security Administration under contract DE-NA0003525. This paper describes objective technical results and analysis. Any subjective views or opinions that might be expressed in the paper do not necessarily represent the views of the U.S. Department of Energy or the United States Government.

A. Reproducing study results

The MATLAB code and data used to reproduce the results presented in this paper are available at <https://github.com/SNL-WaterPower/fbWecCtrl>.

References

- [1] K. Gunn, C. Stock-Williams, Quantifying the global wave power resource, *Renewable Energy* 44 (2012) 296–304.
- [2] Central Intelligence Agency, *The World Factbook 2020*, 2020. URL: <https://www.cia.gov/library/publications/resources/the-world-factbook/>.
- [3] P. T. Jacobson, G. Hagerman, G. Scott, Mapping and assessment of the United States ocean wave energy resource, Technical Report DOE/GO/18173-1, Electric Power Research Institute, 2011. URL: <https://www.osti.gov/servlets/purl/1060943>. doi:10.2172/1060943.
- [4] S. Dasgupta, B. Laplante, C. Meisner, D. Wheeler, J. Yan, The impact of sea level rise on developing countries: a comparative analysis, *Climatic Change* 93 (2009) 379–388.
- [5] K. Schaber, F. Steinke, T. Hamacher, Transmission grid extensions for the integration of variable renewable energies in europe: Who benefits where?, *Energy Policy* 43 (2012) 123–135.
- [6] K. Schaber, F. Steinke, P. Mühlich, T. Hamacher, Parametric study of variable renewable energy integration in europe: Advantages and costs of transmission grid extensions, *Energy Policy* 42 (2012) 498–508.
- [7] W. Sasaki, Predictability of global offshore wind and wave power, *International journal of marine energy* 17 (2017) 98–109.
- [8] M. Hossain, N. Madlool, N. Rahim, J. Selvaraj, A. Pandey, A. F. Khan, Role of smart grid in renewable energy: An overview, *Renewable and Sustainable Energy Reviews* 60 (2016) 1168–1184.
- [9] T. Perez, T. I. Fossen, A Matlab toolbox for parametric identification of radiation-force models of ships and offshore structures, *Modeling, Identification and Control: A Norwegian Research Bulletin* 30 (2009) 1–15.
- [10] J. Salvatore, World energy perspective: cost of energy technologies, Technical Report, World Energy Council, London, United Kingdom, 2013. URL: https://www.worldenergy.org/assets/downloads/WEC_J1143_CostofTECHNOLOGIES_021013_WEB_Final.pdf.
- [11] D. S. Jenne, Y.-H. Yu, V. Neary, Levelized cost of energy analysis of marine and hydrokinetic Reference Models, in: *3rd Marine Energy Technology Symposium (METS 2015)*, Washington, D.C., 2015. URL: <https://www.nrel.gov/docs/fy15osti/64013.pdf>.
- [12] G. Chang, C. A. Jones, J. D. Roberts, V. S. Neary, A comprehensive evaluation of factors affecting the levelized cost of wave energy conversion projects, *Renewable Energy* 127 (2018) 344–354.
- [13] J. Huckerby, H. Jeffrey, A. de Andres, L. Finlay, An international vision for ocean energy, version III, 2016. URL: www.ocean-energy-systems.org.

- [14] V. S. Neary, M. Lawson, M. Previsic, A. Copping, K. C. Hallett, A. LaBonte, J. Rieks, D. Murray, Methodology for Design and Economic Analysis of Marine Energy Conversion (MEC) Technologies., Technical Report SAND2014-9040, Sandia National Laboratories, 2014. URL: <https://energy.sandia.gov/wp-content/gallery/uploads/SAND2014-9040-RMP-REPORT.pdf>.
- [15] J. Hals, J. Falnes, T. Moan, A comparison of selected strategies for adaptive control of wave energy converters, *Journal of Offshore Mechanics and Arctic Engineering* 133 (2011) 031101.
- [16] R. G. Coe, G. Bacelli, D. G. Wilson, O. Abdelkhalik, U. A. Korde, R. D. R. III, A comparison of control strategies for wave energy converters, *International Journal of Marine Energy* 20 (2017) 45 – 63.
- [17] K. Budal, J. Falnes, A resonant point absorber of ocean-wave power, *Nature* 256 (1975) 478–479.
- [18] D. V. Evans, A theory for wave-power absorption by oscillating bodies, *Journal of Fluid Mechanics* 77 (1976) 1–25.
- [19] W. H. Munk, Origin and generation of waves, in: *Proceedings of First Conference on Coastal Engineering*, Long Beach, CA, 1950.
- [20] M. K. Ochi, *Ocean waves: the stochastic approach*, volume 6, Cambridge University Press, 2005. doi:10.1017/CBO9780511529559.
- [21] K. Ogata, *Modern Control Engineering*, volume 4, Prentice Hall, 2002.
- [22] D. J. Inman, *Vibration with control*, John Wiley & Sons, 2017.
- [23] K. Aström, R. Murray, *Feedback Systems: An Introduction for Scientists and Engineers*, Princeton University Press, 2010.
- [24] E. Jefferys, Simulation of wave power devices, *Applied Ocean Research* 6 (1984) 31–39.
- [25] J. Falnes, *Ocean Waves and Oscillating Systems*, Cambridge University Press, Cambridge; New York, 2002.
- [26] A. Price, C. Dent, A. Wallace, On the capture width of wave energy converters, *Applied Ocean Research* 31 (2009) 251 – 259. *Renewable Energy: Leveraging Ocean and Waterways*.
- [27] K. Bubbar, B. Buckham, On establishing generalized analytical phase control conditions in two body self-reacting point absorber wave energy converters, *Ocean Engineering* 197 (2020) 106879.
- [28] G. Bacelli, R. G. Coe, Comments on control of wave energy converters, *IEEE Transaction on Control System Technologies* (2020) 1–4.
- [29] D. M. Pozar, *Microwave engineering*, John Wiley & Sons, 2009.
- [30] S. Silver, *Microwave antenna theory and design*, 19, Iet, 1984.
- [31] J. N. Newman, *Marine hydrodynamics*, MIT Press, Cambridge, Massachusetts, 1978.
- [32] R. G. Coe, G. Bacelli, S. J. Spencer, D. Forbush, K. Dullea, Advanced WEC Dynamics and Controls MASK3 Test, Technical Report SAND2019-15428, Sandia National Laboratories, Albuquerque, New Mexico, 2019. URL: <https://www.osti.gov/biblio/1592850-advanced-wec-dynamics-controls-mask3-test>. doi:10.2172/1592850.
- [33] R. G. Coe, G. Bacelli, D. Forbush, S. J. Spencer, K. Dullea, B. Bosma, P. Lomonaco, FOSWEC dynamics and controls test report, Technical Report SAND2020-XXXX, Sandia National Laboratories, 2020.
- [34] G. Bacelli, R. G. Coe, D. Patterson, D. Wilson, System identification of a heaving point absorber: Design of experiment and device modeling, *Energies* 10 (2017) 472.
- [35] R. Pintelon, J. Schoukens, *System identification: A frequency domain approach*, John Wiley & Sons, 2012.
- [36] L. Ljung, *System identification - Theory for the User*, Prentice-Hall, 1999.
- [37] WAMIT, *WAMIT User Manual*, 7 ed., Chestnut Hill, MA, 2012. URL: <http://www.wamit.com/manual.htm>.
- [38] A. Babarit, G. Delhommeau, Theoretical and numerical aspects of the open source BEM solver NEMOH, in: *Proceedings of the 11th European Wave and Tidal Energy Conference (EWTEC2015)*, 2015. URL: <https://hal.archives-ouvertes.fr/hal-01198800>.
- [39] G. Bacelli, *Optimal control of wave energy converters*, PhD, National University of Ireland, Maynooth, Maynooth, Ireland, 2014. URL: <http://mural.maynoothuniversity.ie/6753/>.
- [40] D. D. Forbush, G. Bacelli, S. J. Spencer, R. G. Coe, A self-tuning WEC controller for changing sea states (in press), in: *Proceedings of the 21st IFAC World Congress*, 2020.
- [41] V. Nevarez, G. Bacelli, R. G. Coe, D. G. Wilson, Feedback resonating control for a wave energy converter, in: *Proceedings of SPEEDAM2018*, 2018. URL: <https://ieeexplore.ieee.org/document/8445379>. doi:10.1109/SPEEDAM.2018.8445379.
- [42] G. Bacelli, V. Nevarez, R. G. Coe, D. Wilson, Feedback resonating control for a wave energy converter, *IEEE Industrial Automation and Control* 56 (2020) 1862–1868.
- [43] D. G. Violini, Y. Peña-Sanchez, N. Faedo, J. V. Ringwood, An energy-maximising linear time invariant controller (LiTe-Con) for wave energy devices, *IEEE Transactions on Sustainable Energy* (2020).
- [44] H. Cho, G. Bacelli, R. G. Coe, Model predictive control tuning by inverse matching for a wave energy converter, *Energies* 12 (2019) 4158.
- [45] M. Lawson, Y.-H. Yu, A. Nelessen, K. Ruehl, C. Michelen, Implementing nonlinear buoyancy and excitation forces in the wec-sim wave energy converter modeling tool, in: *Proceedings of the 33rd International Conference on Ocean, Offshore and Arctic Engineering (OMAE 2014)*, ASME, San Francisco, CA, 2014.
- [46] D. Son, R. W. Yeung, Optimizing ocean-wave energy extraction of a dual coaxial-cylinder wec using nonlinear model predictive control, *Applied Energy* 187 (2017) 746 – 757.
- [47] M. Richter, M. Magana, O. Sawodny, T. Brekken, Nonlinear model predictive control of a point absorber wave energy converter, *Sustainable Energy, IEEE Transactions on* 4 (2013) 118–126.
- [48] M. Penalba, G. Giorgi, J. V. Ringwood, Mathematical modelling of wave energy converters: a review of nonlinear approaches, *Renewable and Sustainable Energy Reviews* 78 (2017) 1188–1207.
- [49] H. Cho, G. Bacelli, R. G. Coe, Linear and nonlinear system identification of a wave energy converter, in: *Proceedings of the 6th Marine Energy Technology Symposium (METS)*, Washington, D.C., 2018. URL: <https://www.osti.gov/servlets/purl/1506194>.
- [50] N. MOSTAGHEL, T. DAVIS, Representations of coulomb friction for dynamic analysis, *Earthquake Engineering & Structural Dynamics* 26 (1997) 541–548.
- [51] S. Salter, J. Taylor, N. Caldwell, Power conversion mechanisms for wave energy, *Proceedings of the Institution of Mechanical Engineers, Part M: Journal of Engineering for the Maritime Environment* (2002).
- [52] J. Perdigo, A. Sarmento, A phase control strategy for OWC devices in irregular seas, in: *Proceedings of the 4th International Workshop on*

- Water Waves and Floating Bodies, volume 205-209, 1989. URL: http://www.iwwwfb.org/Abstracts/iwwwfb04/iwwwfb04_40.pdf.
- [53] J. Hals, Modelling and phase control of wave-energy converters, PhD, Norwegian University of Science and Technology, Trondheim, Norway, 2010. URL: <http://ntnu.diva-portal.org/smash/record.jsf?pid=diva2:403616>.
- [54] D. Valério, P. Beirão, J. S. da Costa, Optimisation of wave energy extraction with the archimedes wave swing, *Ocean Engineering* 34 (2007) 2330–2344.
- [55] H.-N. Nguyen, P. Tona, Continuously adaptive PI control of wave energy converters under irregular sea-state conditions, in: Proceedings of the 12th European Wave and Tidal Energy Conference (EWTEC2017), Cork, Ireland, 2017. URL: <https://hal.inria.fr/hal-01628466/>.
- [56] S. Shi, R. J. Patton, M. Abdelrahman, Y. Liu, Learning a predictionless resonating controller for wave energy converters, in: ASME 2019 38th International Conference on Ocean, Offshore and Arctic Engineering, American Society of Mechanical Engineers Digital Collection, 2019.